

Evidence for blueshift by weak exciton confinement and tuning of bandgap in superparamagnetic nanocomposites

Swapna S. Nair, Mercy Mathews¹, M.R. Anantharaman^{*}

Department of Physics, Cochin University of Science and Technology, Thrikkakkara, Cochin 682 022, Kerala, India

Received 10 December 2004; in final form 17 February 2005

Available online 29 March 2005

Abstract

Superparamagnetic nanocomposites based on $\gamma\text{-Fe}_2\text{O}_3$ and sulphonated polystyrene were synthesised by ion-exchange process and the structural characterisation has been carried out using X-ray diffraction technique. Doping of cobalt in to the $\gamma\text{-Fe}_2\text{O}_3$ lattice was effected in situ and the doping was varied in the atomic percentage range 1–10. The optical absorption studies show a band gap of 2.84 eV, which is blue shifted by 0.64 eV when compared to the reported values for the bulk samples (2.2 eV). This is explained on the basis of weak quantum confinement. Further size reduction can result in a strong confinement, which can yield transparent magnetic nanocomposites because of further blue shifting. The band gap gets red shifted further with the addition of cobalt in the lattice and this red shift increases with the increase in doping. The observed red shift can be attributed to the strain in the lattice caused by the anisotropy induced by the addition of cobalt. Thus, tuning of bandgap and blue shifting is aided by weak exciton confinement and further red shifting of the bandgap is assisted by cobalt doping.

© 2005 Elsevier B.V. All rights reserved.

1. Introduction

Magnetic nanocomposites have gained considerable interest in recent years because of the novel physical properties exhibited by these materials at the nanolevel. [1–4]. The properties of nanostructured materials are determined by a complex interplay of the building blocks and the interfaces [5]. These studies are motivated not only by the interesting properties of these particles at the nanolevel, but also due to the technological applications of magnetic nanoparticles in diverse fields such as in ferrofluids, magnetic recording, catalysis and magnetic refrigeration [6,7]. The design, synthesis and char-

acterisation of nanocomposite materials has become the subject of intense current research.

It is possible to observe quantum size effects at finite temperatures in these ultra fine particles. Their quantum size effects include improved magnetic properties, quantum magnetic tunneling and the shift in the optical absorption edge. Also their large surface to volume ratio provides scope for excellent modification of their physical properties due to the large reduction in linear dimensions and high lattice strain [3,4]. These peculiar properties include their single domain and super paramagnetic nature at the nanolevel [5–7]. Optical properties also change enormously including the band gap due to the small wave function overlapping because of their extremely small sizes comparable to their Bohr radius.

To study the finite size effects of semiconductors, the effect of potential jumps and quantum confinements have to be incorporated. The optical bandgap shifts towards longer wavelength region in the ultra fine regime due to the additional exciton confinement energy.

^{*} Corresponding author. Fax. +91485 2577057.

E-mail addresses: swapna@cusat.ac.in (S.S. Nair), mra@cusat.ac.in (M.R. Anantharaman).

¹ Present address: Systems and Materials for Information Storage Group, University of Twente, PB No. 217, 7500 AE, Enschede, The Netherlands.

As the length parameters of these quasi particles or nanoclusters are noticeably larger than the lattice constant for most of the semiconductors, elementary excitons will experience quantum confinement resulting in finite motion along the confinement axis and infinite motion in other directions.

Gamma ferric oxide belongs to the class of inverse spinels and it exhibits a vacancy ordered spinel structure, where the vacancies are exclusively on the octahedral (B) sites [8]. This material has been extensively used for various applications in the bulk due to its very high saturation magnetisation and remanance especially for audio/video recording. They exhibit novel properties at the nanolevel due to its vacancy ordered structure. The structure of gamma ferric oxide can be written as, $\text{Fe}^{3+}[\text{Fe}_{5/3}^{3+}\square_{1/3}]\text{O}_4^{2-}$, where \square represents vacancies and are exclusively on the octahedral sites.

Nanocomposites can be synthesised by different methods like high energy ball milling (HEBM), sol–gel technique and ion-exchange methods. Of these methods, ion-exchange method is the best in limiting the grain size due to the small pore size available, which are in the nanodimensions. This method also provides least clustered grains.

In the present investigation, nanocomposites were synthesised by ion exchange process and their optical properties have been evaluated. Attempts are made to explain the observed blue shift in the optical bandgap based on the weak quantum confinement of exciton due to their ultrafine grain structure.

In situ doping was carried out on a polystyrene- $\gamma\text{-Fe}_2\text{O}_3$ nanocomposite. Cobalt is a material, which has a strong octahedral site preference, whose introduction in the lattice results in enhanced magnetic properties both in terms of saturation magnetisation and in terms of coercivity. Tuning of magnetic parameters were made possible with the addition of cobalt as the dopant and the results are already published [10]. Attempts are made to tune the optical bandgap of these nanocomposites, over a vast visible region, by the addition of cobalt, which

was never reported to the best of our knowledge. The possibility of making a transparent magnetic composite is bright if one understands the mechanism of strong exciton confinement property in magnetic materials, which finds extensive applications in magneto-optical displays, magnetic field controlled optical modulators, optical switches and magneto-optical actuators.

2. Experimental techniques

2.1. Preparation of magnetic nanocomposites

The samples were synthesised by ion-exchange process using sulphonated polystyrene. Sulphonated polystyrene was used as the ion-exchange resin. Samples were ion exchanged for 24 h with $\text{FeSO}_4 \cdot 7\text{H}_2\text{O}$ and then treated with 1 N NaOH and few drops of 25% H_2O_2 solution. The details are cited elsewhere [9]. The ion-exchange cycling was carried out both at room temperature and at a higher temperature of 65 °C using $\text{FeSO}_4 \cdot 7\text{H}_2\text{O}$ solution. The schematic diagram of a typical ion-exchange process is depicted in Fig. 1.

2.2. Doping

Doping with Co was carried out using the same strong ion-exchange process using $\text{CoSO}_4 \cdot 7\text{H}_2\text{O}$ in the appropriate molar ratio. The details are cited elsewhere [10]. In situ doping was effected in the atomic percentage 1–10%. The cycling was carried out using $\text{CoSO}_4 \cdot 7\text{H}_2\text{O}$ and up to the 10th cycle for each atomic percentage of cobalt.

2.3. XRD studies

The cycled nanocomposites were ball milled in a high energy ball mill in an aqueous medium for which Fritsch Pulverisette 7 Planetary Micro Mill was employed and the samples were dried to obtain them in the powder

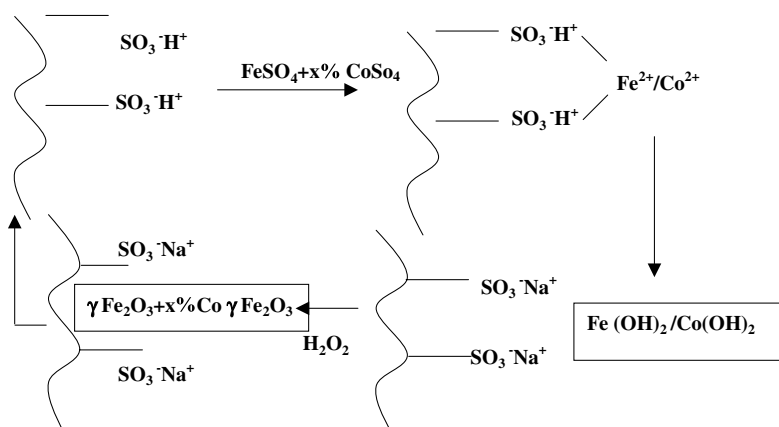


Fig. 1. The schematic diagram of ion-exchange process.

form. The milling time and the speed of rotation were carefully kept very low so as to avoid any structural changes that may be imparted during the high energy ball milling process. The XRD spectra of the samples were recorded on an X-ray diffractometer (Rigaku D-max-C) using Cu K α radiation ($\lambda = 1.5405 \text{ \AA}$). The particle size was estimated by employing Debye–Scherer’s formula,

$$D = \frac{0.9\lambda}{\beta \cos \theta},$$

where λ is the wave length of X-ray used, β is the FWHM in radians of the XRD peak with highest intensity, D is the particle diameter, θ is the glancing angle.

2.4. Iron and cobalt content estimation

The nanocomposite samples were analysed using Atomic Absorption Spectroscopy (AAS) for the determination of the exact percentage of Iron in the samples. From the relative intensities of the absorption lines, the percentage of iron in the polymer globules can be determined. The samples were analysed for each and every cycle of ion exchange in order to determine whether there is an increase in iron content with cycling. The same method was employed for the measurement of exact percentage of cobalt that has gone into the composite sample. Estimation was carried out for samples with Co in the atomic percentage 1, 2, 4, 6 and 10 (atomic percentage of cobalt in $\gamma\text{-Fe}_2\text{O}_3$) for representative ion exchange cycles 1 and 10.

2.5. Preparation of aqueous ferrofluids and thin films

Aqueous ferrofluids were synthesised from these synthesised nanocomposites by high energy ball milling (HEBM) process using Fritsh Pulversite 7 Micromill at a rotational speed of 600 rpm with known amount of water. Thin films were prepared by dip coating method and the parameters like concentration and temperature have been optimised.

2.6. Optical studies

Optical absorption spectrum was recorded using a Hitachi U-3410 UV–VIS–NIR spectrophotometer for the pure as well as cobalt doped samples and the band gap was determined for all the synthesised samples. In order to calculate the band gap (assuming direct band gap), it may be noted that for a semiconductor, the absorption coefficient near the band edge is given by

$$\alpha = \frac{A(h\nu - E_g)^{1/2}}{h\nu},$$

where A is a constant and E_g is the energy band gap. When $\alpha h\nu = 0$, $E_g = h\nu$. So using an extrapolation to

the X-axis of the plot of $(\alpha h\nu)^2$ vs. $h\nu$, gives the bandgap of the material if it is a direct transition which is the Tauc plots [12].

3. Results and discussions

The X-ray diffraction pattern indicates that the composites display semi crystalline characteristic due to the presence of a large polymer content of the host matrix polystyrene and the particle size, calculated by employing Debye–Scherer’s formula, is roughly 70 \AA for all the synthesised samples. The cycling of iron resulted in increase in crystallinity. It may be noted that X-ray diffraction pattern consisted of peaks corresponding to pure $\gamma\text{-Fe}_2\text{O}_3$ and no other impurity peaks were detected. (see Fig. 2).

The estimation of cobalt was carried out using Atomic Absorption Spectroscopy (AAS) and is indicated against the number of Co^{2+} ion-exchange cycling, (Table 1) which shows a saturation of cobalt content at about 10% Co-doped samples. The magnetisation measurements were carried out and are reported elsewhere [10]. This shows an increase in coercivity in accordance with the doping percentage of cobalt. (see Fig. 3).

The optical absorption spectra of the pristine and the doped samples were recorded and their optical bandgaps were determined using Tauc plots. They are shown in

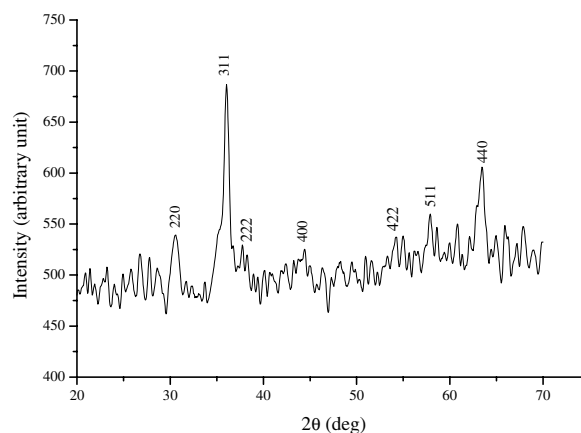


Fig. 2. Representative X-ray diffraction pattern of $\gamma\text{-Fe}_2\text{O}_3$ -polystyrene nanocomposites.

Table 1
Cobalt content intended and estimated

Co in atomic percentage (intended)	As detected by AAS
2	2.1
4	3.6
6	5.6
8	8.2
10	11.1

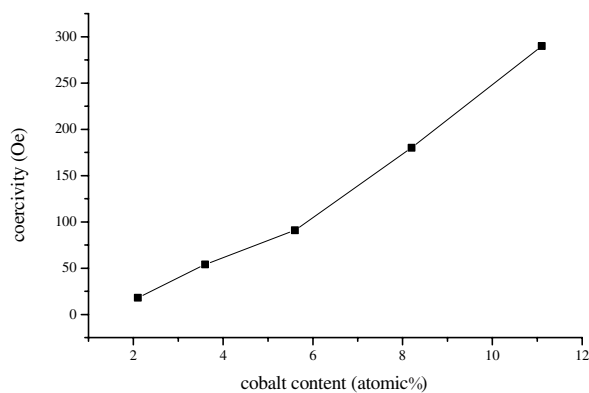


Fig. 3. The variation of coercivity with percentage of Co (as determined by AAS).

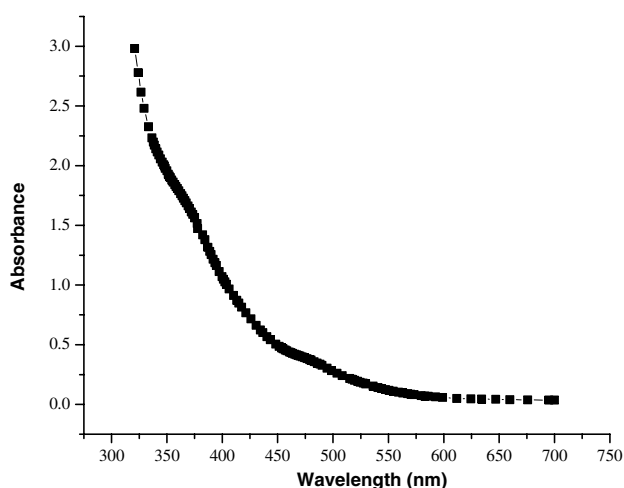


Fig. 4. Absorption spectra of γ -Fe₂O₃-polystyrene nanocomposites.

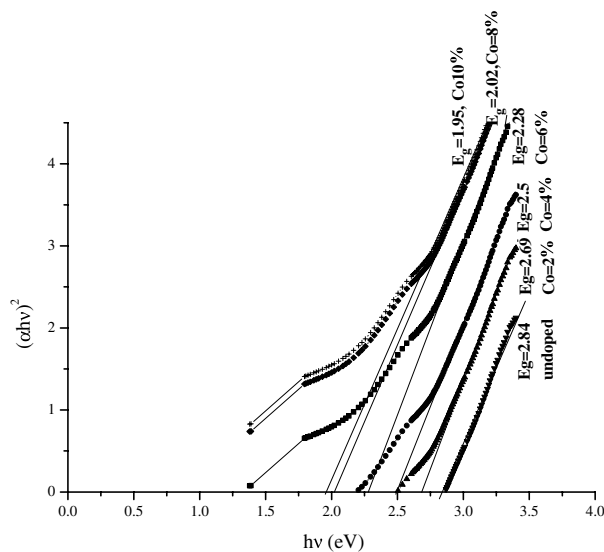


Fig. 5. Optical bandgap determination of the pure as well as cobalt doped samples using Tauc plots.

Table 2
Cobalt content against optical bandgap

Cobalt doping (atomic percentage)	Optical bandgap (eV)
Bulk ^a	2.2
Ultrafine ^b	2.84
2	2.69
4	2.5
6	2.25
8	2.02
10	1.95

^a Bulk γ -Fe₂O₃.

^b Ultrafine γ -Fe₂O₃ in the polymer matrix.

Fig. 5 [11]. A large blue shift of 0.64 eV for the undoped samples ($E_g = 2.84$ eV) is observed as compared to the bulk value. The details are included in Table 2.

Optical absorption spectrum of many of the nanocrystalline semiconductors exhibits a blue shift mainly due to the quantum confinement. The confinement in these nanostructured semiconductors could be broadly divided into two extremes, namely the strong and the weak confinement. In the strong confinement regime, the grain size is less than $2a_0$, where a_0 is the exciton Bohr radius of the material and in the weak confinement regime, the grain size is larger than $4a_0$. In between these limiting cases, both electron and hole confinement and their Coulomb interaction should also be considered.

In the weak confinement regime, quantisation of exciton centre of mass comes into play. Starting from the dispersion law of an exciton in a crystal, the energy of a free exciton is replaced by a solution derived for a particle in a spherical potential well [12]. The energy of an exciton in the weak confinement case is then of the form

$$E_{nml} = E_g - \frac{Ry^*}{n^2} + \frac{\hbar^2 \chi_{ml}^2}{2Ma^2}, \quad (3.1)$$

E_g is the bandgap, ' Ry^* ' is the Rydberg's constant of the hydrogen like exciton, ' χ_{ml} ' is the spherical Bessel function and ' η ' is a constant having the dimension of inverse frequency.

For the lowest state ($n = 1, m = 1, l = 0$) the energy can be expressed as

$$E_{1s1s} = E_g - Ry^* + \frac{\pi^2 \hbar^2}{2Ma^2}, \quad (3.2)$$

which could be rewritten as,

$$E_{1s1s} = E_g - Ry^* \left[1 - \frac{\mu}{M} \left(\frac{\pi^2 a_B^2}{a} \right) \right], \quad (3.3)$$

where μ is the reduced mass of the electron–hole pair. The value $\chi_{10} = \pi$, and the relation for confinement energy becomes,

$$\Delta E_{1s1s} = \frac{\mu}{M} \left(\frac{\pi a_B}{a} \right)^2 Ry^*, \quad (3.4)$$

which is, however, small compared with Ry^* so far as $a \gg a_B$,

holds. This is the quantitative justification of the term ‘weak confinement’.

Taking into account of photon absorption which can create an exciton with zero angular momentum, the absorption spectrum will then consist of a number of lines corresponding to states with $l=0$. therefore, the absorption spectrum can be derived from Eq. (3.1) with $\chi_{m0} = \pi m$

$$E_{nm} = E_g - \frac{Ry^*}{n_2} + \frac{\hbar^2 \pi^2}{2Ma^2} m^2, \quad (3.5)$$

the ‘free’ electron and heavy hole have the energy spectra

$$E_{ml}^e = E_g + \frac{\hbar^2 \chi_{ml}^2}{2m_e a^2}, \quad (3.6)$$

$$E_{ml}^h = \frac{\hbar^2 \chi_{ml}^2}{2m_h a^2}, \quad (3.7)$$

therefore, the total excess energy for the lowest electron and hole in 1s state is

$$\Delta E_{1s1s} = \left(\frac{\pi a_B}{a}\right)^2 Ry^*. \quad (3.8)$$

Or in terms of effective mass of the exciton (electron-heavy hole pair) and grain radius, using Eq. (3.5) confinement energy can be written as

$$E_{sh} = \frac{\hbar^2 \pi^2}{2m_{\text{eff}} R^2}, \quad (3.9)$$

where R is the nanocrystalline radius and m_{eff} is the effective mass of the exciton in weak confinement. Thus confinement energy is clearly a function of the nanoparticle radius and varies as $1/R^2$.

Actually the exciton of 1s electron-heavy hole has comparable values of effective mass m_{eff} for almost all the semiconductors and thus the energy shift variation becomes a function of the nanoparticle radius in the weak confinement regime.

From Eq. (3.9), it could be concluded that mere quantum confinement in the weak regime can itself account for an energy shift of 0.64 eV in the material as compared to the bulk value when the grain size is limited in the size limit of $R = 40 \text{ \AA}$ as calculated by line broadening of the X-ray diffraction spectrum. If the grain size could be further reduced to 40 \AA ($R = 20 \text{ \AA}$), quantum dot confinement can be achieved. This will result in a blue shift up to 1.68 eV. This falls under the regime of strong confinement. Under such circumstances the particles become optically transparent. Hence, the blue shift in the absorption spectrum obtained in pure nanocrystalline $\gamma\text{-Fe}_2\text{O}_3$ could be fitted to the quantum confinement in the weak confinement regime with the reduced mass m_{eff} is $0.6 m_0$ along the longitudinal.

The band gap shows a gradual red shift in the optical absorption edge for the Co-doped samples in comparison with the pure sample and this red shift is in accordance with the doping percentage. The red shift in absorption edge (as compared to the undoped samples) can be attributed to the pressure induced effects [13], which is manifested in nanoparticles and this extreme small size results in an increased surface pressure and hence increased lattice strain which decreases the bandgap as,

$$P = 2\gamma/R, \quad (3.10)$$

where γ is surface tension and P , the pressure due to surface tension and for particle of diameter around 100 \AA , the pressure of 0.4 GPa is calculated. Thus, a red shifted absorption edge can be expected. In undoped samples due to the weak exciton confinement, there is an enhancement of bandgap observed. But the presence of an atom like cobalt with large magneto-crystalline anisotropy increases the total strain effects, which helps in shifting the spectrum towards higher wavelength side, and thus the spectrum gets red shifted and the red shift gets further enhanced with the dopant amount in the lattice.

The pressure induced effects will contribute to the lattice strain and thus results in reduced bandgap. The pressure induced effects is rather very small compared to the actual shift obtained in the doped samples in comparison with the undoped samples. So in order to account for this large red shift, we have to consider the additional intermediate dopant energy levels. This can reduce the bandgap to a considerable amount.

Presence of cobalt at the vacancies of $\gamma\text{-Fe}_2\text{O}_3$ could create energy states in the band gap region that may develop into a narrow energy band as dopant concentration increases. Then the effective gap for transitions between this narrow band and other localised states or the conduction band would then definitely will be smaller than the undoped samples. Also the increase in concentration of the dopants increase the stress anisotropy and its effect on its magnetic properties have been studied and was reported elsewhere [10].

Thus, in nanocrystalline $\gamma\text{-Fe}_2\text{O}_3$ doped with cobalt, two opposing effects determine the shift in band gap. One of them is the weak exciton confinement leading to the blue shifted absorption edge for the undoped samples. But as the dopant concentration increases, due to the large crystalline anisotropy, the stress induced effects comes into play. Also the small energy states formed in between the band gap grows as a narrow band and thus reducing the energy band gap of the material.

In some semiconductors it is reported that [11] the band gap decreases with increase in the pressure and strain induced effects and eventually the band gap closes and the semiconductor undergoes a semiconductor to metal transition at critical pressures which is a factor

determined by the material. Here, nanocrystalline γ -Fe₂O₃ were synthesised with large blue shifted absorption edge with weak exciton confinements, and tuning of both optical and magnetic parameters are effected with the addition of a specific dopant like cobalt, which becomes very important from the application point of view.

4. Conclusion

Absorption edge of ultrafine γ -Fe₂O₃-polystyrene magnetic nanocomposites synthesised by chemical route was blue shifted by an amount of 0.64 eV due to weak exciton confinement. Strong confinement can result in a theoretical blue shift of around 1.45 eV (in a quantum dot confinement); but that may reduce the magnetic properties and thus not favoured under the application point of view. Thus transparent magnetic nanocomposites (in the visible range) could be synthesised by size reduction of the order of the Bohr radius limits, which can throw open a wide field with versatile application potential in magneto-optics. Also tuning of optical bandgap is made possible which is reported for the first time in these magnetic nanocomposites by doping with Co and the spectrum gets red shifted more and more with increased doping and finally gets saturated due to the formation of a complete dopant level in the intermediate (see Fig. 4).

Acknowledgements

M.R.A. and S.S.N. acknowledge the financial assistance provided by the Department of Science and Tech-

nology, Government of India in the form of a project (File No. SP/S2/M-64/96 dated 22/04/2002). M.R.A. is grateful to TWAS, Trieste, Italy (File No. 00-118 RG/PHYS/AS) and IUCDAEF, Mumbai, India. for funding. Fruitful discussions and suggestions from Jinesh K.B., Department of Physics, Leiden University, The Netherlands, Hysen Thomas, and Ajimsha S, Department of Physics, CUSAT, India, are gratefully acknowledged.

References

- [1] R.F. Ziolo, E.P. Giannelis, B.A. Weinstein, M.P. O'horo, B.N. Gganguly, V. Mehrotra, M.W. Russel, D.R. Huffmann, *Science* 219 (1992) 257.
- [2] R.D. Shull, L.H. Bennet, *Nanostruct. Mater.* 1 (1992) 83.
- [3] E.M. Chudnovsky, L. Gunther, *Phys. Rev. B* 37 (1998) 9455.
- [4] R. Gangopadhyay, A. De, *Chem. Mat.* 12 (2000) 608.
- [5] C.P. Bean, J.D. Livingstone, *J. Appl. Phys.* 30 (1959) 120.
- [6] R.D. McMichael, R.D. Shull, L.J. Swartzendruber, L.H. Bennet, R.E. Watson, *J. Magn. Magn. Mater.* 111 (1992) 29.
- [7] K.A. Gscheinder, V.K. Pecharsky, *J. Appl. Phys.* 85 (8) (1999) 5365.
- [8] J. Smit, H.P.J. Wijn, *Ferrites*, Philips technical library, 1959.
- [9] K.A. Mailini, M.R. Anantharaman, S. Sindhu, C.N. Chinnasamy, N. Ponpandian, A. Narayanasamy, B. Balachandran, V.N. Shivasankarapillai, *J. Mater. Sci* 36 (2001) 821.
- [10] S. Swapna Nair, M. Mathews, P.A. Joy, M.R. Anantharaman, *J. Magn. Magn. Mater.* 283 (2–3) (2004) 344.
- [11] R.F. Ziolo, P. Giannelis, R.D. Shull, *Nanostruct. Mater.* 3 (1993) 85.
- [12] R. Turton, *The Physics of Solids*, Oxford University Press, New York, 2000.
- [13] J.K. Vassiliou, V. Mehrotra, M.W. Russel, R.D. Mc Michael, R.D. Shull, R.F. Ziolo, D.K. Smith, C. Mailhlot, *Rev. Mod. Phys* 62 (1990) 173.